Ilmenite ($FeTiO_3$) is a suitable mineral to produce titanium dioxide (TiO_2) for photocatalyst applications. Therefore, this research was conducted to synthesize TiO_2 material from titanium oxysulfate ($TiOSO_4$) extracted from Indonesia local ilmenite mineral ($FeTiO_3$) and to modify this material into TiO_2 nanotubes through a hydrothermal process at 150 °C for 24 hours followed by a post-hydrothermal treatment with temperature variations of 80, 100, 120, and 150 °C for 12 hours. The purpose was to investigate the effect of the post-hydrothermal variations on the crystal structure, morphology, and optical properties of the TiO_2 nanotubes produced. It was discovered from the scanning electron microscopy (SEM) observations that the TiO_2 nanotube was successfully derived from the ilmenite precursor. Moreover, the X-Ray diffraction (XRD) analysis of the nanotube crystal structure showed that post-hydrothermal treatment enhanced the crystallinity of the anatase TiO_2 phase even though the sodium titanate phase was observed to exist in the structure. The increase in the post-hydrothermal temperature from 80 to 150 °C was also discovered to have led to:

1) a reduction in the unit cell volume from 136.37 to 132.31 $Å^3$ and a decrease in the lattice constant c from 9.519 to 9.426 Å;

2) an increase in density from 7.783 to 8.081 gr/cm^3 as well as in the crystallite size from 19.185 to 25.745 nm;

3) a decrease in the bandgap energy (Eg), from 3.33 to 3.02 eV.

These characteristics further indicate the ability of the photocatalytic performance of the nanotubes to enhance the degradation efficiency from 87.69 to 97.11 %. This means the TiO_2 nanotubes extracted from local $FeTiO_3$ can provide the expected crystal structure and photocatalytic performance

Keywords: TiO_2 nanotube, post-hydrothermal, crystallite size, bandgap energy, photocatalytic, ilmenite mineral

UDC 621.793
DOI: 10.15587/1729-4061.2022.255145

SYNTHESIS OF TITANIUM DIOXIDE NANOTUBE DERIVED FROM ILMENITE MINERAL THROUGH POST-HYDROTHERMAL TREATMENT AND ITS PHOTOCATALYTIC PERFORMANCE

Ahmad Fauzi
Doctor of Engineering, Doctoral Student*
Latifa Hanum Lalasari
Doctor of Engineering, Senior Researcher
Research Center for Metallurgy
National Research and Innovation Agency (BRIN)
Kawasan Puspiptek GD 470, Tangerang Selatan, Indonesia, 15314
Nofrijon Sofyan
Doctor of Engineering, Associate Professor*
Alfian Ferdiansyah
Doctor of Engineering, Junior Lecturer*
Donanta Dhaneswara
Doctor of Engineering, Associate Professor*
Akhmad Herman Yuwono
Correspondind author
Doctor of Engineering, Professor*
E-mail: ahyuwono@eng.ui.ac.id
*Department of Metallurgical and Materials Engineering
Universitas Indonesia (UI)
Kampus UI, Jalan Margonda Raya, Pondok Cina, Beji,
Kota Depok, Jawa Barat, Indonesia, 16424

Received date 01.03.2022
Accepted date 07.04.2022
Published date 29.04.2022

How to Cite: *Fauzi, A., Lalasari, L. H., Sofyan, N., Ferdiansyah, A., Dhaneswara, D., Yuwono, A. H. (2022). Synthesis of titanium dioxide nanotube derived from ilmenite mineral through post-hydrothermal treatment and its photocatalytic performance. Eastern-European Journal of Enterprise Technologies, 2 (12 (116)), 15–29. doi: https://doi.org/10.15587/1729-4061.2022.255145*

1. Introduction

The development of the textile industry in Indonesia is experiencing rapid growth in line with the community's increasing needs. In 2018, the development of the textile industry experienced an increase in exports by 6 %. This increase is expected to continue to grow and reach 13–14 billion US$ in the following years. The number of textile companies also increased from 2,880 to 2,980, by 3.5 percent (Indonesian Textile Association). But on the other hand, it turns out that this harms the environment, namely the increasing amount of textile waste that is difficult to degrade in water media. Therefore, there is an urgent need for a textile waste treatment process to overcome this problem and thus minimize environmental pollution. This is currently conducted through several conventional techniques such as chlorination [1], ozonation [2], biodegradation [3], and absorption processes [4], which require high operational costs, thereby making it difficult for them to be implemented. The search for a more economic and environmental alternative led to the consideration of the photocatalytic technique as the solution for the current and future problems in textile waste treatment.

One of the semiconductor materials often used in photocatalytic processes is titanium dioxide (TiO_2) [5] due to its chemical stability, non-toxicity, pollution-free, photochemical corrosion resistance, and relatively low price. However, this material has certain limitations, which include the low optical response in visible light illumination and fast electron-hole pair recombination, which can reduce the

pollutant degradation rate [6]. Several techniques have been used to overcome these problems such as the doping [7] and modification of TiO_2 morphology from nanoparticles to nanotubes [8, 9]. One-dimensional (1-D) nanostructures including nanotubes have been considered one of the ideal nanostructures for photocatalytic applications.

TiO_2 nanotubes can be formed through the basic hydrothermal procedure using TiO_2 treated with an aqueous solution of 10 M NaOH for 20 h at 110 °C [10]. The basic hydrothermal procedure has been adopted in our previous research where TiO_2 nanotubes were synthesized from the commercial precursor of P25 Degussa TiO_2 nanoparticles with the application of additional pre-annealing and post-hydrothermal treatments on the samples [11]. The variation of the pre-annealing and post-hydrothermal treatment temperatures was discovered to have significantly enhanced the nanocrystallinity of the anatase TiO_2 phase in the nanotubes while the integrity of the tubular nanostructures was well-maintained.

However, it was realized that the procurement of P25 Degussa TiO_2 requires quite tedious importing line procedures, thereby leading to limited stock and expensive price. This means there is an urgent need to find an alternative TiO_2 precursor from nearby local resources. Therefore, the ilmenite ($FeTiO_3$) mineral from Bangka Island, Indonesia is considered to have great potential due to its TiO_2 content with 30–65 % purity accompanied by other oxides compounds [12, 13]. Several processing steps are required to convert the ilmenite mineral into TiO_2 and these can be achieved through the pyrometallurgical [14] and hydrometallurgical [15] extraction routes. In this extraction process, the hydrometallurgical route is often used to optimize the formation of TiO_2 nanoparticles. The ilmenite extraction through the hydrometallurgy process for obtaining titanium dioxide precursor and its conversion into TiO_2 nanotubes via hydrothermal and post-hydrothermal treatments are the main concerns in the current investigation. Therefore, studies in this work are selecting the best variables in the metallurgical extraction process with sulfate pathway, starting with the decomposition process using sodium hydroxide, and washing with sulfuric acid at low concentrations to obtain titanium oxosulphate ($TiOSO_4$), which are subjected to hydrolysis process for the formation of TiO_2 particles. Further hydrothermal process by dissolving the resulting TiO_2 particles with NaOH at a low temperature of around 150 °C with a relatively long time of about 24 hours can change the TiO_2 nanostructure from nanoparticles to nanotubes. The function of the post-hydrothermal process is to increase the crystallinity of TiO_2 nanotubes and maintain their hollow structure integrity.

2. Literature review and problem statement

The paper [16] presents the results of research about natural titanium dioxide nanotubes. Titanium dioxide nanotubes are based on ilmenite-leucoxene ores through a hydrothermal process. The process dissolves 0.8 g of ilmenite-leucoxene ores with 10 M NaOH, then puts it in an autoclave tightly closed and put in an oven at a temperature of 110 °C for 24 hours. It was concluded that the hydrothermal process resulted in the synthesis of TiO_2 nanotubes having an outer diameter of 70–100 nm, a larger surface area of 230 m^2/gr, and smaller bandgap energy of 2.4 eV, and the photocatalytic performance was no less good than that of commercial precursor nanotubes. In this study, the extraction process was not carried out, so there were still many impurities in titanium dioxide. The direct precursor of ilmenite-leucoxene ores was obtained by a hydrothermal method without any extraction process, and crystallinity calculations were not carried out. There are unresolved problems related to the extraction process and crystallinity that have not been considered. All this indicates that it is advisable to carry out an extraction process to obtain TiO_2 nanoparticles, and a process that can get higher crystallinity is carried out.

The paper [9] presents the results of research about the synthesis of titanium dioxide nanotubes via a one-step dynamic hydrothermal process. Synthesis of titanium dioxide nanotubes using commercial TiO_2 powder. The effects of NaOH concentration, reaction time, reaction temperature, stirring process, and washing on the morphology and the exchange ions of the nanotubes were investigated. It can be concluded that the dynamic hydrothermal process, stirring conditions affected the yields and structural uniformity of the nanotubes. The Na^+ ions attached to the nanotubes are obliterated by HCl aqueous solution and deionized water treatments. Moreover, during the dynamic hydrothermal process, the nanotubes were obtained, which contradicts the assumption that titanate precursor sheets would only scroll after acid treatment. This study still uses commercial precursors, so it has limitations related to limited stock and high costs. The photocatalytic performance test has unresolved issues about precursor and crystallinity that have not been considered. All of this indicates that it is advisable to use natural precursors to be cheaper and easier to obtain, and a process that can get higher crystallinity is carried out.

The paper [17] presents the results of research about Nanocrystaline Titanium Dioxide Nanotube (TDN) by Hydrothermal Method From Tulungagung Mineral Sand. Synthesis of titanium dioxide nanotubes using the Tulungagung Mineral Sand precursor, which was carried out by hydrometallurgical extraction process with sulfate pathway at 120 °C. Then the filtrate was hydrolyzed at 200 °C to obtain TiO_2 powder precipitate. TiO_2 powder was dissolved with NaOH, then put into an autoclave, heated in an oven at 130 °C for 24 hours, and continued with the acid and water washing treatment process to obtain a TiO_2 nanotube structure. It can be concluded that the results obtained are single-phase anatase TiO_2 nanotubes with a crystallite size of 43.99 nm. In this study, the diffraction peaks from XRD still show low crystallinity, so it is possible to have high bandgap energy. There are unresolved issues related to low crystallinity and no photocatalytic performance test yet. All this indicates that it is advisable to carry out a treatment process to increase crystallinity.

The paper [18] presents the results of research about the Effect of reaction time on the formation of TiO_2 nanotubes prepared by the hydrothermal method. Synthesis of titanium dioxide nanotubes using a commercial precursor, namely titanium tetra isopropoxide (TTIP), which was carried out hydrothermally at 150 °C with a time variation of 10 hours and 16 hours, followed by washing with 0.1 M HCl acid and followed by an annealing process to obtain TiO_2 nanotube powder. It can be concluded that the anatase and rutile TiO_2 phases were obtained from the increased hydrothermal reaction time. The phase change occurs due to the increase in hydrothermal reaction time. TiO_2 nanotubes have a diameter and length of about 11.23 nm and 260 nm and have band-

gap energy at hydrothermal reaction times of 10 hours and 16 hours of about 3.6 eV and 3.5 eV. There are unresolved issues regarding precursors, crystallinity has not been taken into account, and photocatalytic performance tests have not yet been carried out. This indicates that it is advisable to use natural precursors and carry out a process that can obtain higher crystallinity, thereby lowering the bandgap energy.

The paper [19] presents the results of research about the synthesis, characterization and photocatalytic activity of TiO_2 nanostructures: Nanotubes, nanofibers, nanowires and nanoparticles. Synthesis of TiO_2 nanotubes, nanofibers, and nanowires was performed by the hydrothermal treatment of TiO_2 nanoparticles with different NaOH concentrations (5, 10, and 12 N) at 120, 140, and 180 °C. It can be concluded that the bandgap energies of nanotubes, nanofibers, nanowires, nanoparticles, and Degussa P-25 are 3.18, 3.00, 3.10, 3.09, and 3.21 eV because the bandgap energy shows the central performance in the ability to produce OH^- groups thereby increasing their photocatalytic activity. This research, especially TiO_2 nanotubes, still uses commercial precursors, so availability is limited, and costs are expensive. There are unresolved issues regarding precursors and crystallinity. All this indicates that it is advisable to use natural precursors and carry out a treatment process to obtain higher crystallinity.

The paper [20] presents the results of research about the synthesis of stable TiO_2 nanotubes: effect of hydrothermal treatment, acid washing and annealing temperature. TiO_2 nanotubes were synthesized using a commercial precursor P25 Degussa by dissolving it with 10 M NaOH. The solution was put into an autoclave and then heated in an oven at 110 °C for 72 hours. The resulting product was washed with 0.1 M hydrochloric acid and water until the pH was neutral. The samples were dried at 80 °C for 24 hours, followed by an annealing process at 400, 600, and 800 °C for 2 hours. It can be concluded that the effect of hydrothermal treatment and acid washing is significant to form the structure of TiO_2 nanotubes. Hydrothermal treatment can modify TiO_2 nanoparticles from the anatase phase to the monoclinic phase, a characteristic of TiO_2 nanosheet structure. The acid washing process forms nanotubes with high purity because Na^+ ions are exchanged from the titanate structure into HCl solution. At 400 °C, annealing temperature can maintain a stable tube morphology. In comparison, annealing above 600 °C can change the tube morphology structure to become irregular. It can change the crystallinity from anatase to rutile phase, causing damage to the nanotube structure. There are unresolved issues regarding commercial precursors that need to be replaced with natural precursors, crystallinity can still be improved, and photocatalytic performance tests have not yet been carried out. All this indicates that it is advisable to use natural precursors and carry out a process that can obtain higher crystallinity to improve photocatalytic performance.

The paper [21] presents the results of research about the synthesis and Characterization of Single-Layer TiO_2 Nanotubes. Synthesis of TiO_2 nanotubes using the Degussa P25 anatase nanopowder precursor. Synthesis of nanotubes started with 0.5 g TiO_2 was hydrothermally treated with 10 M NaOH aqueous solution and 20 ml of ethanol in a 50 ml stainless steel Teflon-lined autoclave. The mixture was heated in an oven at 180 °C for 24 h. The product was washed with acid and water to obtain a neutral pH, then dried at 80 °C for 4 h, and then calcined at 250 °C for 6 h. It can be concluded that TiO_2 nanotubes (TNTs) have a single uniform layer with an open-ended crystal structure and a uniform tubular shape. TNTs have lengths from 400 to 700 nm and a thickness of 1.07 nm with uniform tubes. TNT has a bandgap energy of 3.0 eV. The ethanol solvent causes a smaller bandgap energy value. This research is still using a commercial precursor, namely P25 Degussa. It is necessary to find an alternative substitute for this precursor due to limited availability and is expensive. There are unresolved issues regarding precursors, crystallinity has not been taken into account, and photocatalytic performance tests have not yet been carried out. All this indicates that it is advisable to use natural precursors and carry out a process that can obtain higher crystallinity.

All of this indicates that it is advisable to conduct research using natural precursors from local Indonesian ilmenite minerals to obtain TiO_2 particles and their subsequent conversion into nanotube structures and nanotubes to have high crystallinity, low bandgap energy, and well-maintained hollow structures, the treatment process is carried out. Post-hydrothermal. Based on these references, the authors decided to form TiO_2 nanotubes using natural precursors and carry out a post-hydrothermal treatment process at different temperatures on the synthesized TiO_2 nanotubes to increase their crystallinity, decrease their bandgap energy values, and obtain the expected photocatalytic performance.

3. The aim and objectives of the study

The aim of the study is to obtain TiO_2 nanotubes from ilmenite mineral precursor, which can function as a suitable photocatalytic material for liquid pollutant degradation.

To achieve the aim, the following objectives are set-up:

– to investigate the effect of post-hydrothermal treatment with temperature variation of 80, 100, 120 and 150 °C for 12 hours on the crystallinity, morphology and bandgap energies of the synthesized TiO_2 nanotubes;

– to correlate the characteristics and properties of nanotubes and their photocatalytic activity performance.

4. Materials and methods

The raw material used in this research was local precursor $FeTiO_3$ extracted from Bangka Island, Indonesia. Several other additional materials used include sodium dioxide (NaOH) (Merck®), sulfuric acid (H_2SO_4) (Merck®), hydrochloric acid (HCl) (Merck®), and aquadest.

The first stage was crushing the ilmenite with a disk mill to a size of 100 mesh and then decomposing it with 30 ml of 10 M NaOH solution in a Teflon-coated autoclave reactor and putting in an oven at 150 °C for 3 hours. The product decomposition is carried out by the sulfate pathway leaching process with 9 M sulfuric acid (H_2SO_4) and the stirring process at 300 rpm at 90 °C for 3 hours to produce a solution of $TiOSO_4$.

The second step was the hydrolysis process where it was dissolved in water at an $H_2O/TiOSO_4$ volume ratio (v/v) of 4:1. This mixture solution was further stirred at a speed of 300 rpm for 2 hours at 90 °C, and later treated under a condensation process for 12 hours at room temperature without stirring in order to obtain white precipitates containing TiO_2 nanoparticles. After that, TiO_2 nanoparticles were analyzed using X-Ray diffraction (XRD) (Shimadzu XRD-7000) to

determine the structural properties of TiO_2 nanoparticles, scanning electron microscopy (SEM) (JEOL-JSM 6390A) to determine the morphology of TiO_2 nanoparticles.

The third step was the modification of nanoparticles into TiO_2 nanotubes through the hydrothermal method [10]. The process was started by dissolving 1 gram of TiO_2 nanoparticle product dissolved into 30 ml of 10 M NaOH solution. The solution was put into a Teflon-coated autoclave and tightly closed and placed in an oven at 150 °C for 24 hours. The product was washed with 0.1 M HCl solution and washed again with distilled water until the pH value became neutral. Subsequently, annealing was carried out at a temperature of 150 °C for 6 hours followed by post-hydrothermal treatment at a temperature variation of 80, 100, 120, and 150 °C for 12 hours. The resulting TiO_2 nanotubes were analyzed using X-Ray diffraction (XRD) (Shimadzu XRD-7000) to determine the structural properties of TiO_2 nanotubes. The crystallite sizes of TiO_2 nanotubes were estimated using Scherrer's equation [22]. The crystal structure analysis was conducted with lattice parameters, unit cell volume, and density using General Structure Analysis System (GSAS) software while crystal model simulation was conducted through Vesta software. Scanning electron microscopy (SEM) (JEOL-JSM 6390 A) was performed to determine the morphology of TiO_2 nanotubes while the optical properties were analyzed using a UV-Vis spectrophotometer (UV-1601, Shimadzu). Furthermore, the optical bandgap energy (E_g) was estimated using Tauc's procedure [23].

The last step was photocatalytic testing of TiO_2 nanotubes by evaluating the percentage of degradation of Methylene Blue (MB). This means 0.25 gram TiO_2 nanotube catalyst was dispersed in 150 ml of MB solution at 5 ppm concentration, stirred with a magnetic stirrer, and placed under a 70 Watt UV radiation lamp for 2.5 hours to measure the photocatalytic activity. The absorption spectrum of the MB solution was recorded every 30 minutes of irradiation after which the photocatalytic degradation was calculated using the efficiency degradation equation [24]. The MB concentration was measured using a UV-Vis spectrophotometer (UV-1601, Shimadzu). While the reaction rate constants for photocatalytic reaction in the liquid phase were determined using the reaction kinetics in the Langmuir-Hinshelwood model [25].

5. Results of TiO_2 nanotubes derived from ilmenite extraction

5. 1. Effect of post-hydrothermal temperature

5. 1. 1. Morphology of nanostructures

Fig. 1, *a*, *b* show the SEM images of TiO_2 material after the hydrolysis process of $TiOSO_4$ solution as well as those related to TiO_2 nanotubes after the hydrothermal process while Fig. 2 depicts the nanotubes after post-hydrothermal treatment at 80, 100, 120, and 150 °C for 12 hours.

It was discovered that TiO_2 material produced from the hydrolysis process of $TiOSO_4$ had an observable nanoparticle structure in the form of small balls piled up such grapes as indicated in Fig. 1, *a*. Meanwhile, TiO_2 changed from a spherical shape to an elongated shape as observed in the long tube threads piled on top of each other in the form of dried nanotubes after the hydrothermal process as presented in Fig. 1, *b*. Moreover, the nanotube structure appears shorter when treated with the post-hydrothermal process at 80 °C as indicated in Fig. 2, *a* and became invisible when the temperature was increased to 100 °C as shown in Fig. 2, *b* but maintained looked like long tube threads stacked on top of each other such spider webs at 120 °C as presented in Fig. 2, *c*. However, the nanotubes appeared short again at 150 °C as indicated in Fig. 2, *d*. Interestingly, it is possible to maintain the *t* morphology of TiO_2 nanotubes in an elongated or shorter form after the post-hydrothermal processing.

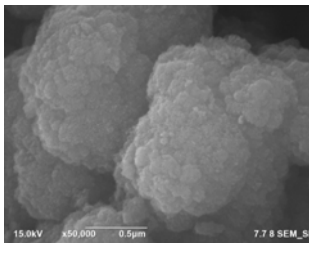

a

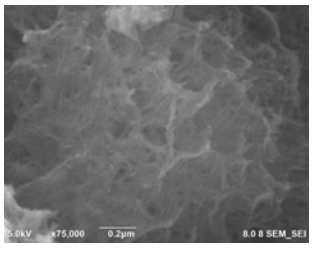

b

Fig. 1. Scanning electron microscopy (SEM) images of: *a* — TiO_2 particles after hydrolysis process of $TiOSO_4$ solution; *b* — TiO_2 nanotubes after the hydrothermal process

SEM figures of TiO_2 nanotubes were further measured to determine the diameter and length. The data were obtained repeatedly up to N=70 using ImageJ software after which the diameter and tube length distribution was analyzed using Origin software. Moreover, fitting analysis was used to provide the R-Square value with the condition that the closeness of the value to 1 indicates the diameter and length of the nanotubes are statistically uniform. The results showed that the best R-square values for the samples of TiO_2 (hydrolyzed), PoHT 100, and PoHT 150 were 0.975, 0.997, and 0.974, respectively as indicated in Table 1, and this means the samples had a uniform diameter. Meanwhile, the results of the diameter distribution in each sample are also presented in Fig. 3.

Additional important information is provided in Fig. 4 to show the R-square value of tube lengths distribution for the hydrothermal and post-hydrothermal PoHT 80, PoHT 120, and PoHT 150 samples. The best results were recorded for hydrothermal product and PoHT 150 samples with 0.975 and 0.909, respectively, as shown in Table 1 and this confirms the uniformity of the tube length.

Table 1

Value of R-Square Diameter and Length of TiO_2 samples

Sample	R-Square Value Diameter	R-Square Value Length
TiO_2 particles after hydrolysis process	0.975	–
TiO_2 nanotubes after hydrothermal process	0.867	0.975
PoHT 80	0.896	0.887
PoHT 100	0.997	–
PoHT 120	0.815	0.867
PoHT 150	0.974	0.909

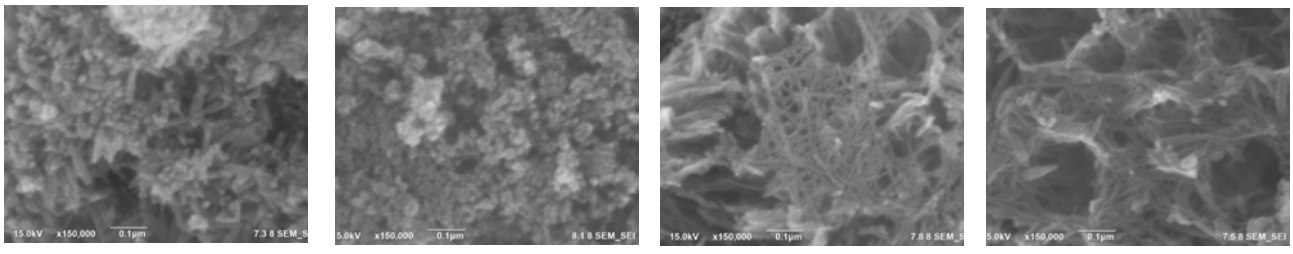

a *b* *c* *d*

Fig. 2. Scanning electron microscopy figures of TiO_2 nanotubes after post-hydrothermal treatment at: *a* – 80; *b* – 100; *c* – 120; *d* – 150 °C

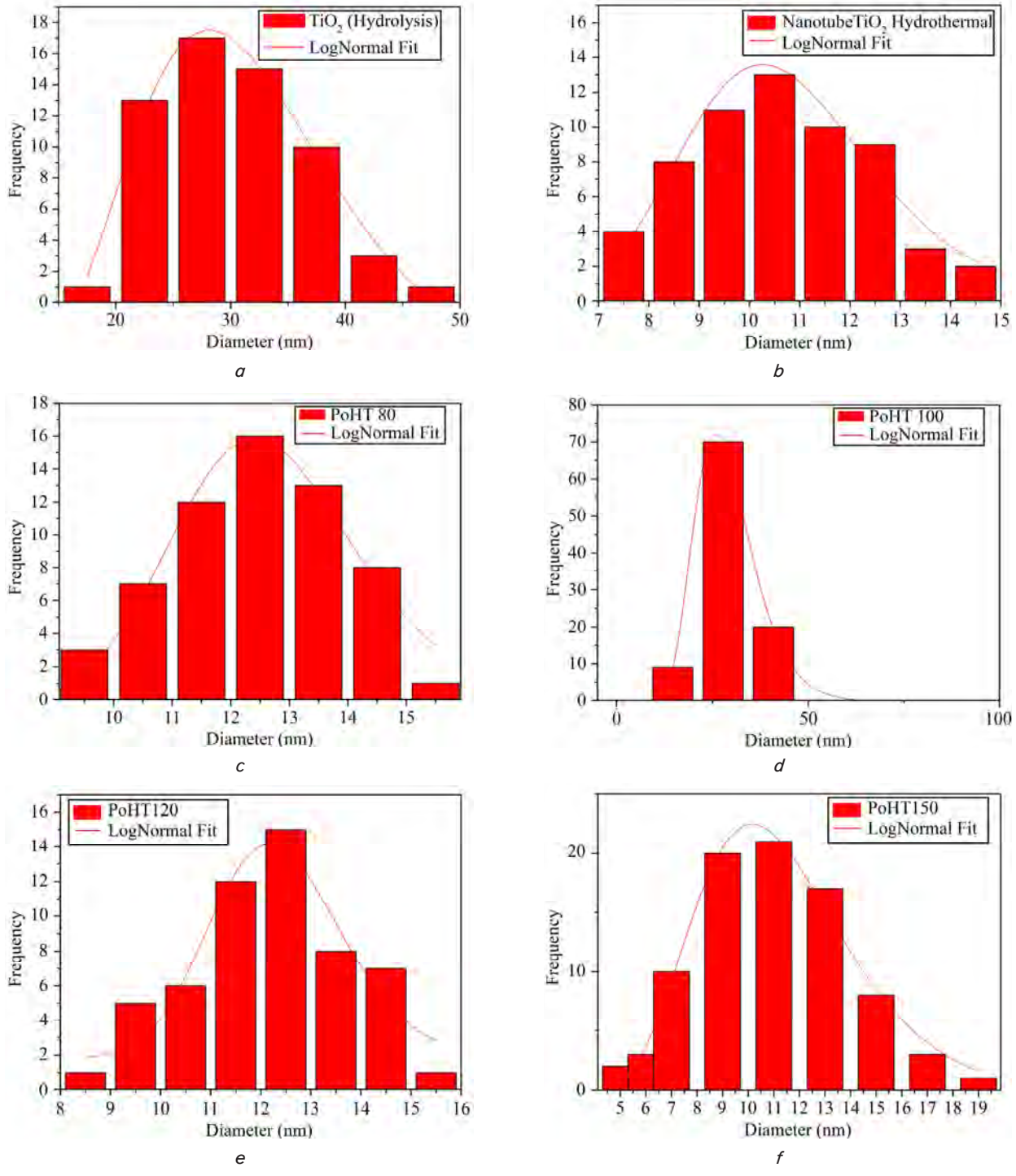

Fig. 3. The results of the diameter distribution of samples: *a* – TiO_2 particles after hydrolysis process; *b* – TiO_2 nanotubes after the hydrothermal process, and TiO_2 nanotubes after post-hydrothermal treatment at: *c* – 80; *d* – 100; *e* – 120; *f* – 150 °C

The other quantitative measurement of the average diameter and length of nanotubes is presented in Table 2. It was discovered that the average diameter of the initial material, the hydrolyzed spherical TiO_2, was found to be 30.73±0.44 nm but the shape was converted into a pipe-like form by the hydrothermal treatment with an average length of 118.83±1.71 nm and a smaller diameter of 10.17±0.14 nm. Meanwhile, the post-hydrothermal treatment at 80 °C enlarged the diameter to 12.43±0.17 nm and decreased the tube length to 86.38±1.26 nm while an increase in the temperature to 100 °C had an adverse effect on the morphology by returning to the original nanoparticle shape with a diameter of 28.73±0.44 nm. A further increase in the temperature to 120 and 150 °C returned the morphology back to the nanotubes and the integrity of the hollow shape was well-maintained.

The composition of the constituent elements of TiO_2 nanotubes after post-hydrothermal was analyzed by EDX (Fig. 5). There are four elements found in TiO_2 nanotubes, namely Ti, O, Na and Fe with compositions of 74.5, 22.7, 2.6 and 0.1 at %, respectively. This shows that the TiO_2 nanotube sample from the ilmenite precursor still contains Fe as an element that provides indirect doping in the TiO_2 nanotube. This is also reinforced by the results of the EDX mapping that there are 4 elements, namely Ti, O, Na and Fe elements with mapping colors brown, blue, purple and red (Fig. 6).

Table 2

Diameter and length of TiO_2 nanotubes

Sample	Diameter (nm)	Length (nm)	Morphology
TiO_2 particles after hydrolysis process	30.730.44	–	Nanoparticles
TiO_2 nanotubes after the hydrothermal process	10.170.14	118.831.71	Nanotubes
PoHT 80	12.430.17	86.381.26	Nanotubes
PoHT 100	28.230.40	–	Nanoparticles
PoHT 120	12.740.22	118.681.61	Nanotubes
PoHT 150	11.380.16	78.281.14	Nanotubes

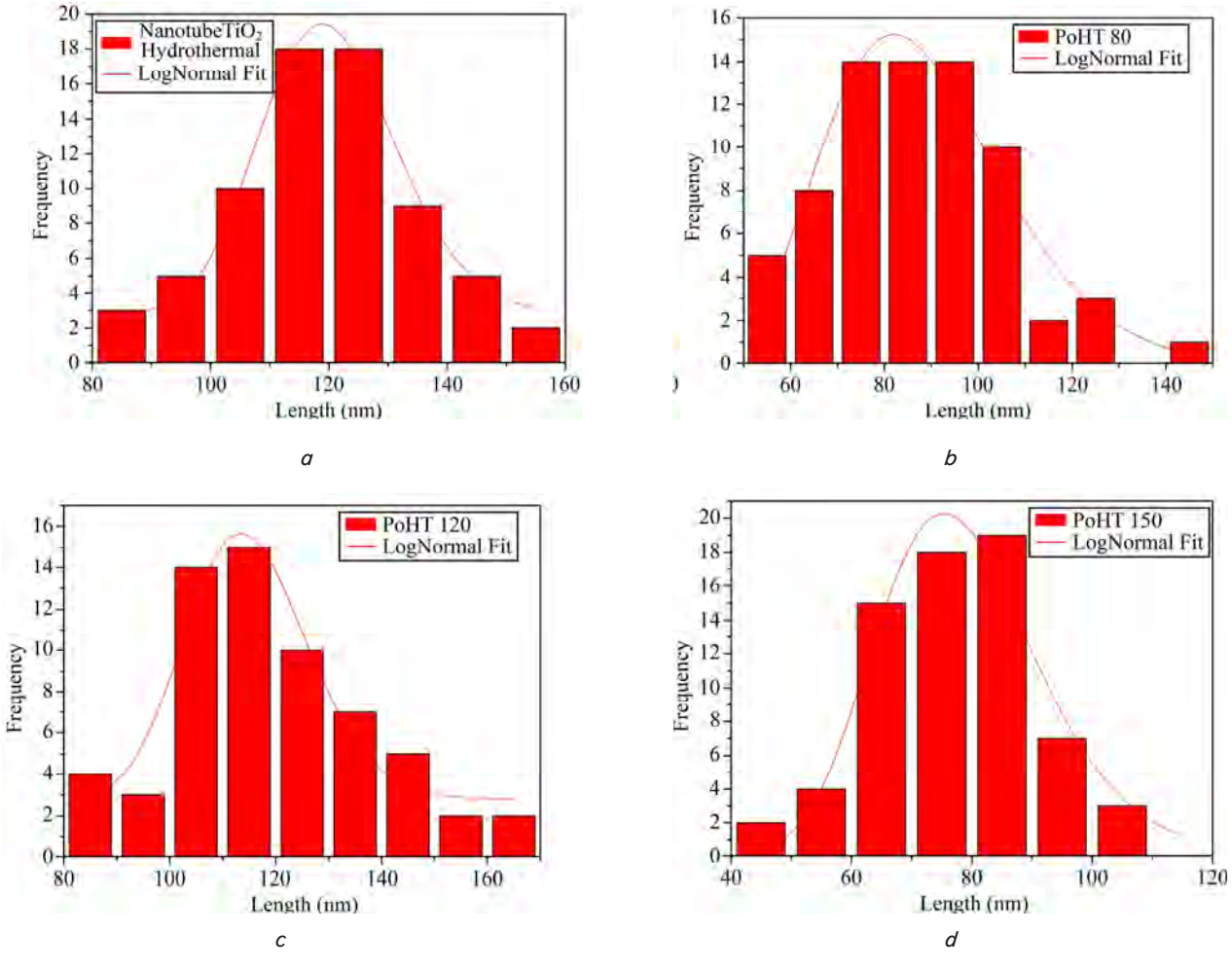

Fig. 4. The length distribution of the samples: *a* – TiO_2 nanotubes after the hydrothermal process and TiO_2 nanotubes after post-hydrothermal treatment at: *b* – 80; *c* – 120; *d* – 150 °C

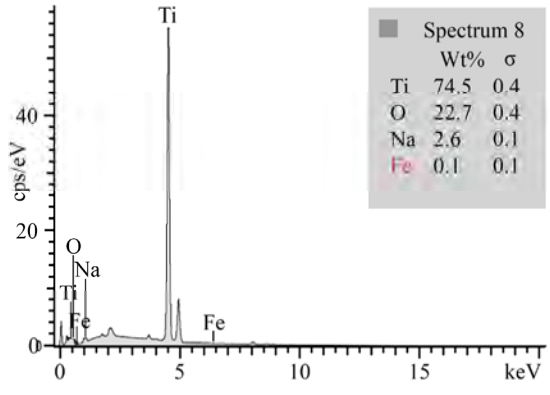

Fig. 5. Energy dispersive X-ray (EDX) analysis of TiO_2 nanotube samples after post-hydrothermal treatment

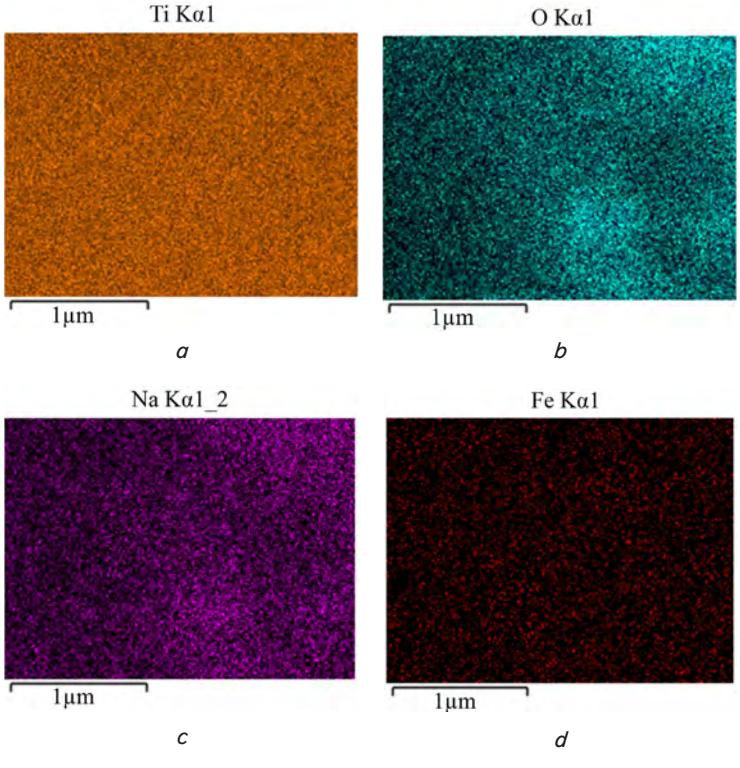

Fig. 6. Energy dispersive X-ray (EDX) mapping of TiO_2 nanotube samples after post-hydrothermal treatment: *a* — Ti; *b* — O; *c* — Na; *d* — Fe

5. 1. 2. Crystal Structure

The XRD pattern of the hydrolyzed TiO_2 sample presented in Fig. 7, *a* indicated only one small diffraction peak at 2θ of 48.0°. This peak belonged to the (200) crystal plane of the anatase TiO_2 phase as confirmed with COD (Crystallography Open Database) no 7206075 [26]. This means the $TiOSO_4$ precursor, which is the product of ilmenite extraction, was already successfully converted into TiO_2 even though its crystallinity was rather low and the XRD pattern of the hydrolyzed TiO_2 sample also contains a minor phase of Fe_2O_3, which is indicated by a diffraction peak at 2θ from 68.6°. It means that there is still Fe_2O_3 impurity. In addition, the hydrothermal process conducted with NaOH facilitated the modification of the structure into nanotube formation. The presence of the sodium titanate phase was also indicated by three diffraction peaks located at 2θ of 27.9, 36.0, and 53.5° as presented in Fig. 7, *b* and these are associated with the (003), (201), and (151) crystal lattice planes as confirmed with COD no 2011660 [43]. Meanwhile, the existence of the anatase TiO_2 phase was observed to have only one diffraction peak at 2θ of 25.3°, which belongs to the (101) crystal plane while the previous (200) vanished and there was also a minor Fe_2O_3 phase, which showed a diffraction peak at 2θ of 68.6°.

The formation of the sodium titanate phase in the nanotubes occurs in the acid washing treatment process, which will break the Ti-O-Ti bond [27]. The process was initiated with the breaking of the Ti-O-Ti bond in the TiO_2 anatase phase to construct a new structure containing Ti-O-Na and Ti-OH bonds once the sodium titanate phase was formed with the exchange of Na^+ with H^+ ions observed to have occurred during the washing process with HCl. This ion exchange provided surface tension variations that caused the titanate layer to peel off, thereby forming unstable nanosheets, which eventually rolled up to produce nanotube structures [28].

Fig. 7, *c–f* show the XRD pattern for nanotube samples post-hydrothermally treated at different temperatures of 80, 100, 120, and 150 °C, and the results showed that the anatase TiO_2 phase became more pronounced as the temperature increased from 80 to 150 °C. This was clearly indicated with the (101) crystal lattice plane, which was more enhanced intensity at 2θ by 25.3° as well as the appearance of new additional peaks of anatase at 2θ by 37.8, 48.0, 55.1, and 62.7° associated with (112), (200), (211), and (204) crystal lattice planes. The intensities were also increased as the post-hydrothermal temperature increased and this was accompanied by the disappearance of sodium titanate (003) and (201) diffraction peaks at 2θ of 27.9 and 36.0 °C even though the peak at 2θ, which was 53.5°, belonged to sodium titanate (151) plane remained upon post-hydrothermal treatment up to 150 °C. The results of the XRD pattern for post-hydrothermal nanotube samples followed by the minor phase are Fe_2O_3. This means that the presence of a minor phase such as Fe_2O_3 provides indirect doping on the TiO_2 nanotubes. Table 3 provides the data extracted from the diffraction peaks of the post-hydrothermally treated samples providing the FWHM value and the estimated crystallite size by using Scherrer's equation. The data shows that the increase in post-hydrothermal temperature from 80 to 150 °C enhanced the crystallite size of the TiO_2 anatase phase from 19.19 to 25.75 nm.

Further crystal structure analysis was conducted on the XRD data using the Rietveld refinement method with GSAS software. The procedure involved inputting raw data in RAW files, crystallographic background data in cif files, and parameters in prm files.

The Powplot results from the GSAS software were indicated by the fit (fitting) of the X-ray diffractogram intensity between the red dotted line, which shows the observation data, the green line, which represents the calculated data, and the pink line, which shows the difference between the two. It was discovered from the two red dotted

lines and the green line that the data coincide as indicated in Fig. 8. This means the XRD data are in accordance with the crystallographic data (COD) of TiO_2 anatase considering the fact that the observation and calculation data match each other.

The refinement analysis was conducted based on the value of goodness of fit (GOF), which shows the conformity between the observed and calculated data. The best GOF value parameter should be close to 1.9 [29] and those recorded for all nanotube samples were found to be lesser than 1.9, thereby indicating they are very close to the ideal target. This means the observed and standard crystallographic databases are a very good match and this confirmed the fitting as indicated in Table 4. The other purification parameters such as residue profile (Rp) and weighted residue profile (wRp) were also used to determine the quality of the refinement as indicated by their values, which are close to 10 % as presented in Table 4. This also confirms that the calculated and observed data are close to the ideal.

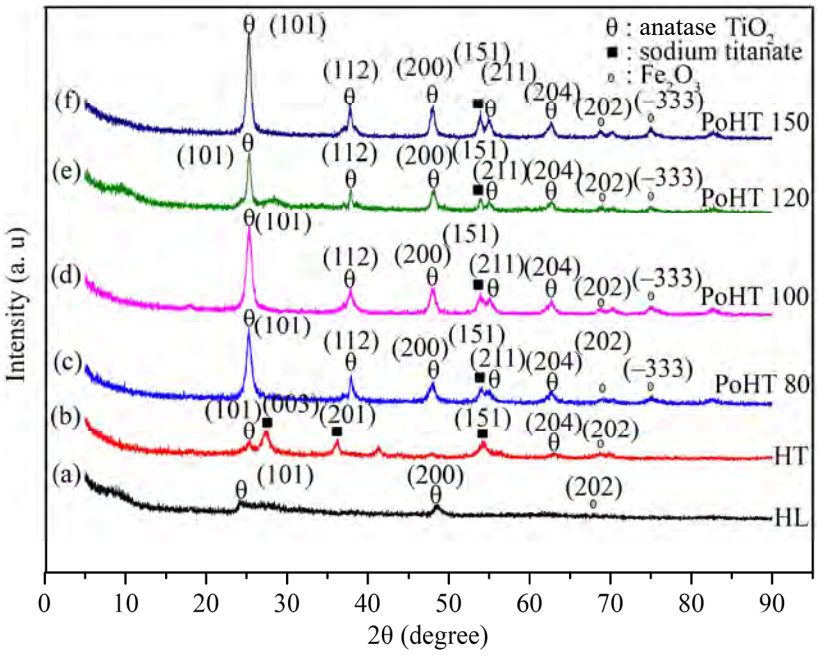

Fig. 7. X-Ray diffraction (XRD) pattern on samples: *a* — TiO_2 particles after hydrolysis process; *b* — TiO_2 nanotubes after the hydrothermal process and TiO_2 nanotubes after post-hydrothermal treatment at: *c* — 80; *d* — 100; *e* — 120; *f* — 150 °C

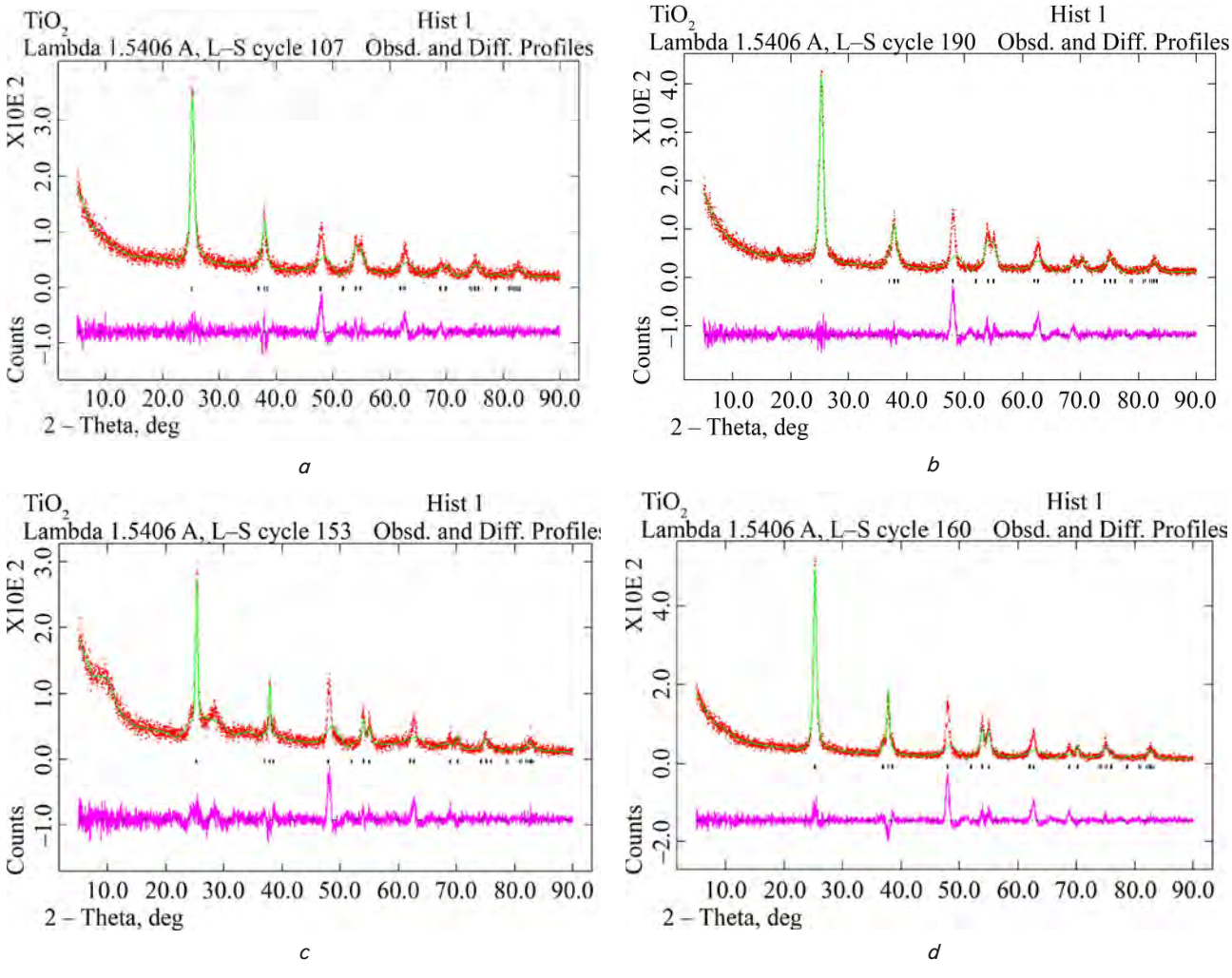

Fig. 8. The Rietveld refinement results for the XRD pattern of post-hydrothermally-treated TiO_2 nanotubes at: *a* — 80; *b* — 100; *c* — 120; *d* — 150 °C

Table 3

The estimated crystallite size of post-hydrothermally-treated TiO_2 nanotubes

Sample	*hkl*	2 Theta (°)	FWHM	*L* (nm)	*L Average* (nm)
PoHT 80	101	25.3	0.2676	30.10	19.19
	112	37.8	0.4684	17.7	
	200	48.0	0.6022	14.28	
	211	55.1	0.6022	14.63	
PoHT 100	101	25.3	0.4349	18.52	22.45
	112	37.8	0.2676	31.0	
	200	48.0	0.4015	21.41	
	211	55.1	0.4684	18.83	
PoHT 120	110	25.3	0.2342	34.38	22.55
	101	37.8	0.2676	31.0	
	200	48.0	0.5353	16.0	
	211	55.1	1.0169	8.71	
PoHT 150	101	25.3	0.3346	24.05	25.75
	112	37.8	0.3346	24.82	
	200	48.0	0.2676	32.15	
	211	55.1	0.4015	21.95	

The quality of a good refinement repair is determined by the slope value of the standard probability plot curve. It was discovered that the value for each sample was 1.03, 1.10, 1.05, and 1.14 and these are almost close to 1.0 while the intercepts of these values were recorded to be 0.08, 0.10, 0.09, and 0.10 of the curve figures, respectively. This led to the formation of linear straight lines as indicated in Fig. 9, thereby proving that the quality of the refinement fittings is close to ideal. This means the refinement was successfully conducted and the ideal value was obtained.

The fitting results of the post-hydrothermally-treated TiO_2 nanotube samples were further refined to determine the lattice parameters, unit cell volume, and density using the GSAS software (Table 5). The reference used for the analysis includes the crystallographic data of TiO_2 anatase with lattice parameters $a=b=3.785$ Å, $c=9.519$ Å, $c/a=2.515$ Å and unit cell volume $V=136.38$ Å^3 as stated by COD 7206075 [26].

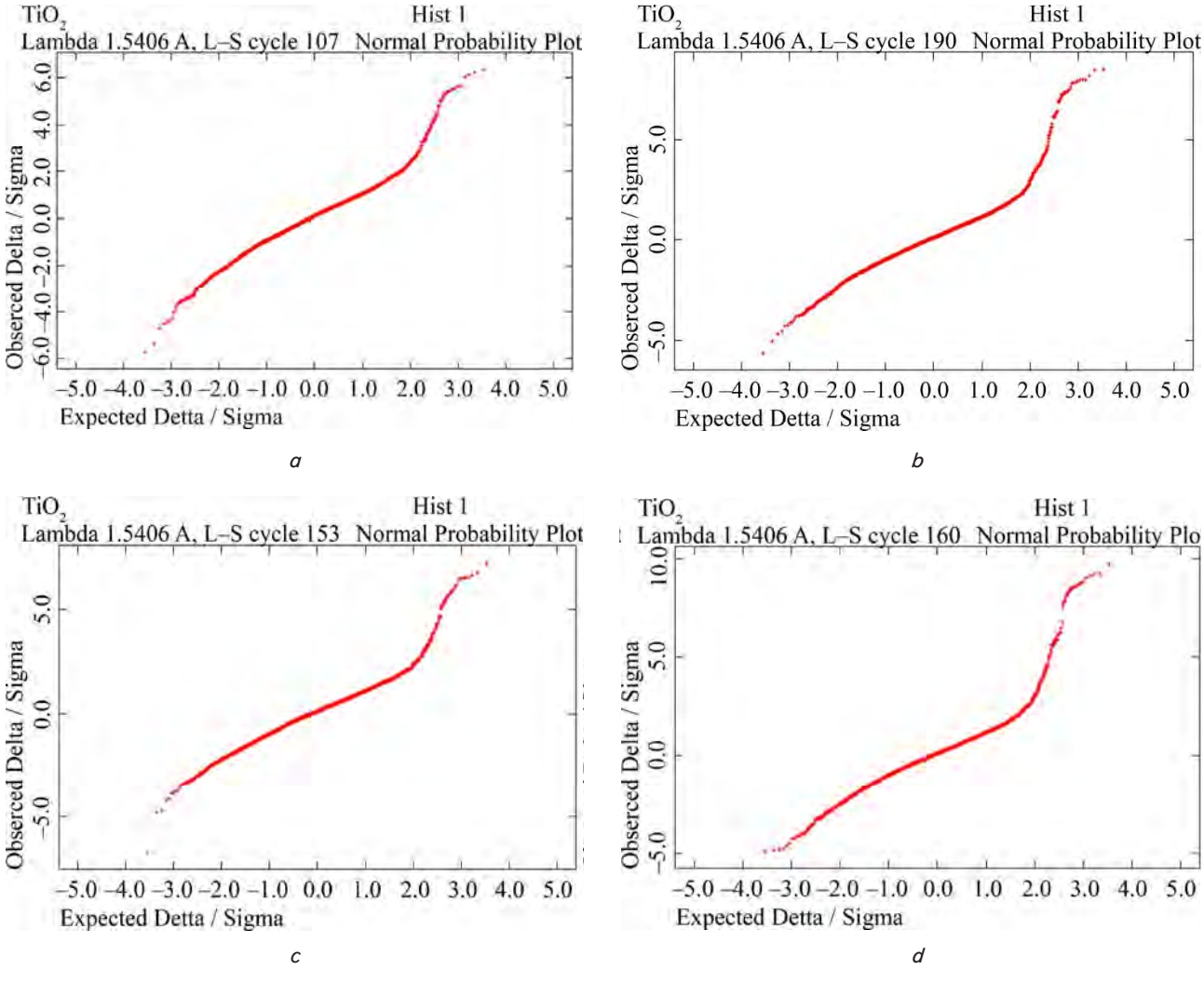

Fig. 9. Normal probability plot curve for Rietveld refinement on the post-hydrothermally-treated TiO_2 nanotubes at: *a* – 80; *b* – 100; *c* – 120; *d* – 150 °C

Table 4

The Rietveld refinement results of post-hydrothermally-treated TiO_2 nanotubes

Sample	Goodness of fit (χ^2)	Residual profile (Rp) %	Weighted residual profile (wRp) %
PoHT 80	1.333	11.91	16.32
PoHT 100	1.742	14.02	20.33
PoHT 120	1.394	12.89	17.76
PoHT 150	1.962	14.89	21.39

Table 5

Lattice parameters obtained from the XRD data refinement of the post-hydrothermally-treated TiO_2 nanotubes

Sample	a (Å)	b (Å)	c (Å)	c/a (Å)	V (Å^3)	ρ (gr/cm^3)
PoHT 80	3.785	3.785	9.519	2.514	136.37	7.783
PoHT 100	3.785	3.785	9.515	2.513	136.29	7.787
PoHT 120	3.784	3.784	9.514	2.514	136.25	7.790
PoHT 150	3.746	3.746	9.426	2.516	132.31	8.081

The results obtained from the refinement showed that the increase in the post-hydrothermal temperature from 80 to 150 °C led to a reduction in the lattice constant c from 9.519 to 9.426 Å and a subsequent reduction in the unit cell volume from 136.37 to 132.31. Therefore, this changed the location and distance between the atoms to approach each other and caused the atomic density to change from 7.783 to 8.081 gr/cm^3.

5. 1. 3. Optical Properties

Fig. 10 shows the UV-Vis spectra of the TiO_2 nanotube samples and the increase in the post-hydrothermal temperature from 80 to 150 °C was observed to have caused the nanotubes to absorb more photon energy as indicated by the red-shift of the absorption edge from 399 to 487 nm. It is important to note that these absorption edge data were further processed to obtain the value of bandgap energy (E_g) of the samples.

Fig. 11, *a–d* show the Tauc's plot of post-hydrothermally-treated samples with the $(\alpha h\nu)^2$ placed on the y-axis while photon energy ($h\nu$) is on the x-axis. Moreover, the E_g value produced by extrapolating the linear part of the curve to the x-axis was 3.33, 3.25, 3.11, and 3.02 for the samples at 80, 100, 120, and 150 °C, respectively. The decrease in the bandgap energy value was observed to be due to the growth of TiO_2 nano-crystallite from 19.19 to 25.75 nm as indicated by the XRD analysis.

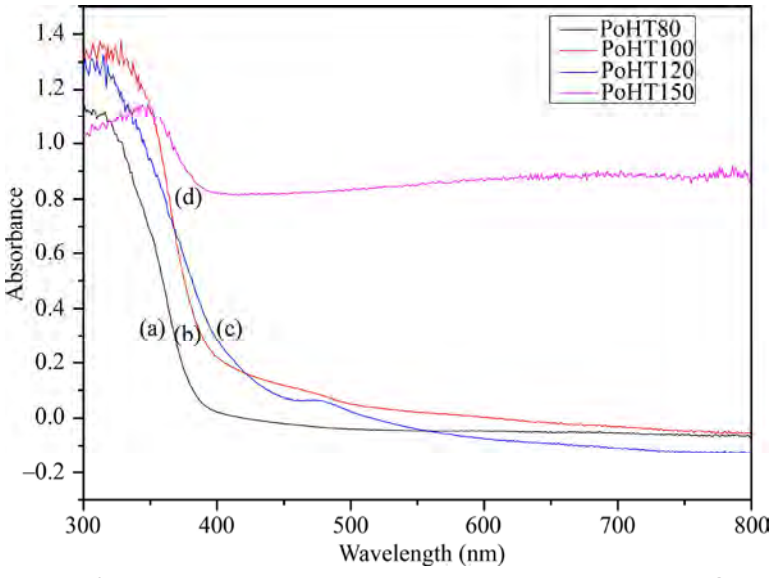

Fig. 10. The absorbance spectra of post-hydrothermally-treated TiO_2 nanotubes at: *a* – 80; *b* – 100; *c* – 120; *d* – 150 °C

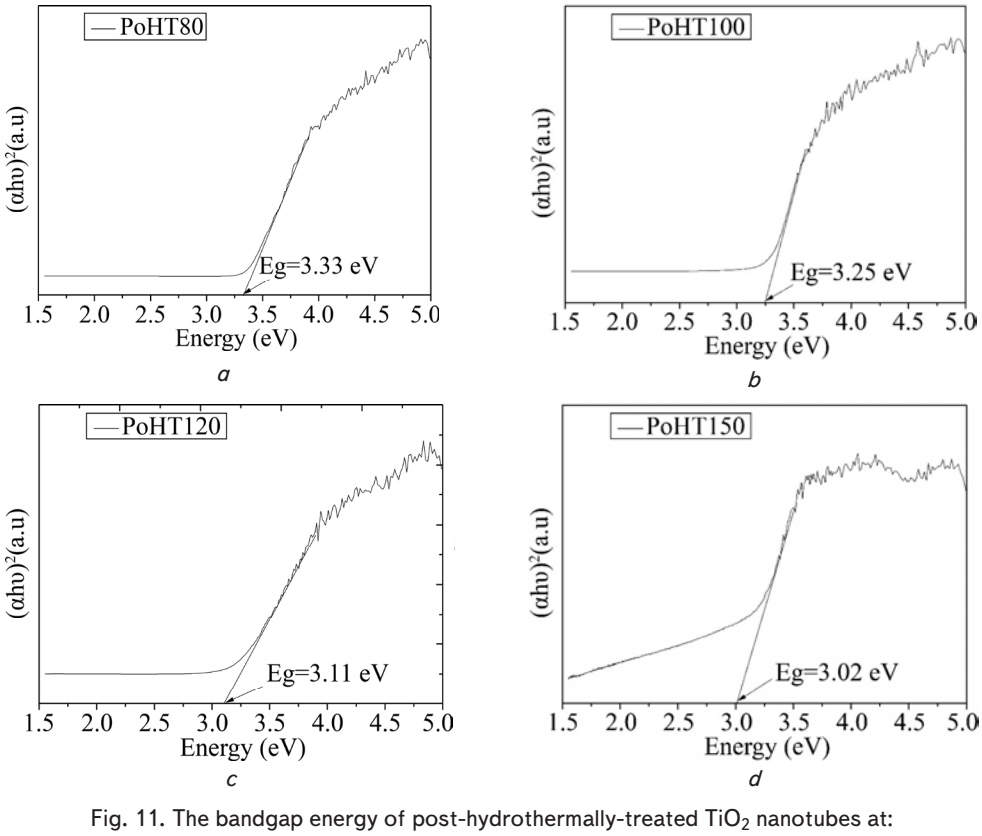

Fig. 11. The bandgap energy of post-hydrothermally-treated TiO_2 nanotubes at: *a* – 80; *b* – 100; *c* – 120; *d* – 150 °C

The same phenomena have been discovered in the previous investigation conducted on post-hydrothermally-treated

TiO_2 nanotubes derived from the commercial precursor P25 Degussa [28]. Moreover, it is well-known that TiO_2, which is one of the semiconductor nanostructures in the nanometer range, shows a change in the bandgap energy value, which is significantly affected by the crystallite sizes. This is observed from the fact that a bigger crystallite has a lower bandgap as indicated in the findings of the previous research on the conventionally-annealed and post-hydrothermally-treated TiO_2 nanoparticles derived from the sol-gel process [30]. It is also interesting to note that the bandgap energies of the samples treated post-hydrothermally at 80 and 100 °C in the present research were found to be closer to those associated with the anatase bulk values of TiO_2, which was 3.20 eV while those treated at 120 and 150 °C produced smaller values of 3.11 and 3.02 eV. The latter results can be explained by the findings of the XRD analysis that the sodium titanate minor phase was also present in the nanotubes in addition to the expected anatase phase. The study [31] showed that sodium titanate has an indirect band gap of 2.99 eV and this means its presence in the TiO_2 nanotubes has a high possibility of narrowing the bandgap space. Furthermore, another possibility was that the iron ions from the $FeTiO_3$ precursor also contributed to the decrease in the bandgap energy due to the presence of Fe ions in TiO_2. It is believed that the interaction of the 3d orbitals of Ti and the d orbitals of Fe metal has the ability to create an intra-band gap state, which causes a decrease in the bandgap energy [32]. It is also important to note that the radius of Fe^{3+}, 0.79 Å, which is similar to Ti^{4+}, 0.75Å, allowed the easy incorporation of Fe^{3+} into the TiO_2 crystal lattice [33]. Meanwhile, the Fe ion substituted has the ability to inhibit the recombination of electrons from the conduction band to the valence band, thereby increasing the photocatalytic activity.

The results of the UV-Vis spectroscopy and estimated bandgap energies calculation were further used to analyze the photocatalytic performance of organic pollutant degradation of the nanotubes as described in the following section.

5. 2. Results of Photocatalytic Activity of TiO_2 Nanotube

5. 2. 1. Degradation efficiency

The photocatalytic performance of the post-hydrothermally-treated nanotubes was analyzed by comparing the MB concentration after UV irradiation for 150 minutes (C_t) with the initial value before irradiation (C_o). The results of the UV-irradiated MB degradation test showed a color change, which was then analyzed with a UV-Vis spectrometer. These results were calculated to obtain the value of photocatalytic activity by comparing the final concentration with the initial concentration of MB, a kinetic reaction model to show the rate of degradation, and the efficiency of degradation to show how significant the percentage of MB degradation was. All these values can be shown in Table 6. The results are also presented in graphical form. The graph can be seen in Fig. 12, *a–c*. The results presented in Fig. 12, *a* showed that all the nanotube samples were able to degrade the MB concentration upon UV irradiation. Moreover, the C_t/C_o value was observed to decrease from 0.12 to 0.03 min^{-1} for nanotube samples post-hydrothermally treated from 80 to 150 °C.

It is also important to note that the final MB concentrations had a similar trend with the E_g values where the higher temperature was discovered to have led to lower E_g values for the samples as indicated by UV-Vis spectroscopy analysis. These lower E_g values allowed the easy facilitation of the electron excitation to the conduction band, thereby leading to an enhanced photocatalytic process by the nanotubes.

The quantitative analysis was conducted using the Langmuir-Hinshelwood model to provide an overview of the photocatalytic degradation rate of MB in TiO_2 nanotubes. The initial MB photocatalytic degradation was caused by the comparatively first-order kinetics-controlled mass transfer due to low target pollutant concentrations as demonstrated by the linear plot of ln $(C_t)/C_o$ versus photocatalytic reaction time (t) in Fig. 12, *b*. The graph also showed that the estimated k value of the post-hydrothermally-treated TiO_2 nanotubes at 150 °C was 0.03307 min^{-1}, which is faster than 0.01816 min^{-1} recorded for 80 °C.

Moreover, the results of the photocatalytic degradation efficiency (η) calculated for all the nanotube samples presented in Fig. 12, *c* showed that an increase in post-hydrothermal temperature from 80 to 150 °C was able to enhance the degradation efficiency significantly from 87.69 to 97.11 %. It is important to note that all the data from the analysis conducted in Fig. 12, *a–c* are summarized in Table 6.

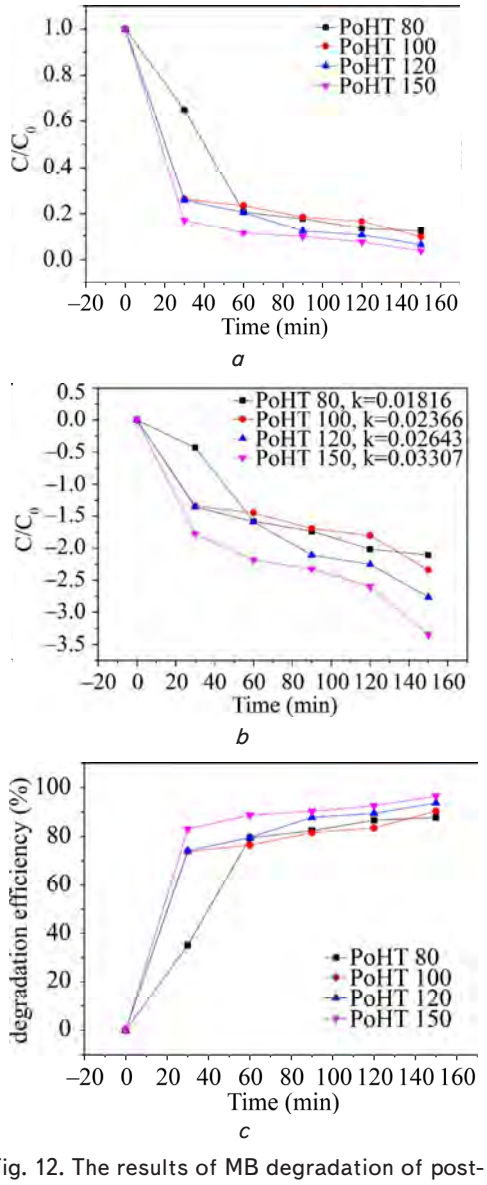

Fig. 12. The results of MB degradation of post-hydrothermal-treated TiO_2 nanotube samples: *a* — photocatalytic activity; *b* — plot of ln $(Ct)/C_o$ versus photocatalytic reaction time (t); *c* — degradation efficiency

Table 6

The summary of the photocatalytic activity, reaction kinetic model, and degradation efficiency on post-hydrothermally-treated TiO_2 nanotubes

Sample	C_t/C_o (min^{-1})	ln $(Ct)/C_o$) (min^{-1})	Degradation efficiency (%)
PoHT 80	0.12	0.01816	87.69
PoHT 100	0.09	0.02366	90.54
PoHT 120	0.05	0.02643	93.42
PoHT 150	0.03	0.03307	97.11

6. Discussion of experimental results of synthesizing titanium dioxide nanotube derived from ilmenite mineral

In this work, the initial step carried out was converting the ilmenite mineral into titanium dioxide through the sulfate extraction process. The extraction result in the form of titanium oxosulphate was subjected to the hydrolysis process, resulting in TiO_2 particles in the nanometer scale as shown in Fig. 1, *a*. The ratio of water to $TiOSO_4$ precursor solution determines the extent of TiO_2 particle size shrinks to nano size upon this hydrolysis process where the more water is added, the more formation of $TiO(OH)_2$ core, which will produce TiO_2 nanoparticles after the drying process [34, 35]. Further modification from nanoparticles into nanotubes was realized through the subsequent hydrothermal process (Fig. 1, *b*). The effect of high temperature and pressure during this process makes the liquid grain boundaries of TiO_2 particles attacked by a strong alkaline NaOH solution [35]. This results in the breakdown of the Ti-O-Ti structure chain of the TiO_2 powder so that the lattice edge of the anatase plane was released to form nanosheets. The nanosheets will roll up and then form the structure of nanotubes as a result of acid washing treatment. This acid washing removes the electrostatics from the residual charge, where Ti-O-Na is converted to Ti-OH, which in turn changed into the nanotubes during the dehydration of the Ti-OH bond.

Via this procedure, several factors can affect the formation of TiO_2 nanotubes including the particle size of the precursor, NaOH concentration, hydrothermal temperature and duration, and post-treatment processes with acid washing and calcination [36, 37]. In our study, the TiO_2 nanotubes were further subjected to post-hydrothermal treatment, involving the use of high-pressure water vapor at various temperatures. With a post-hydrothermal temperature of 80 °C, the treatment has produced nanotubes with short lengths (Fig. 2, *a*). This is due to the applied water vapor that affected the Ti-O-Ti network so that the structure becomes smaller during tube formation. When the post-hydrothermal treatment at 100 °C was applied, however, the higher-pressure water vapor has caused an adverse effect on the arrangement of the Ti-O-Ti network resulting in damage to the tube structure (Fig. 2, *b*). Water vapor can have a positive effect on the structure of the Ti-O-Ti network in an environment with high humidity levels at temperatures above 100 °C [38]. Therefore, in our current study, it was found that the samples subjected to the post-hydrothermal treatment at 120° and 150 °C have shown the well-maintained integrity of the nanotube structure and at the same time their TiO_2 phase crystallinity was significantly enhanced (Fig. 2, *c*, *d*). The crystallinity improvement during the application of post-hydrothermal treatment is resulted from the cutting mechanism by the high-pressure water vapor molecules on the rigid Ti-OH network to form much a more flexible Ti-O-Ti bond, which is in turn capable of rearranging and fully densifying TiO_2 phase of high crystallinity. The above results have demonstrated the effectiveness of high-pressure water vapor in increasing the crystallinity of TiO_2 nanotubes while preserving their hollow structure. This has been confirmed with the XRD results in Fig. 7 with a significant increase in the diffraction peak for the (101) crystal plane. This study shows that the crystal plane (101) of the TiO_2 bulk material, the involvement of water molecules in the cleavage mechanism of the Ti-O-Ti rigid network play an important role in rearrangement for the formation of nanocrystalline TiO_2 [39]. The results of the involvement of water molecules in the cleavage mechanism of the Ti-O-Ti rigid network and their rearrangement into nanocrystalline TiO_2.

The current works with XRD still reveal the presence of iron (Fe) element containing phase in the resulted nanotubes. This can not be avoided since during the extraction process, the addition of iron powder was not carried out. This is normally performed in order to reduce Fe^{3+} ions into the dissolved Fe^{2+} ions, which can precipitate together with TiO_2. However, this condition provided an advantage where the remaining iron ions function as a dopant to provide a donor level so that the photon energy required for electrons to excite from the valence band to the conduction band decreases. This mechanism works together with the enhanced nanocrystallinity of the TiO_2 phase causing the bandgap energy of the TiO_2 nanotubes to approach the bulk anatase value of TiO_2 as shown in Fig. 11. The synergizing condition facilitates the expected photocatalysis performance of the TiO_2 nanotubes.

The photocatalytic activity was expressed by the percentage of methylene blue degradation, as shown in Fig. 12, *c*. Indeed, the photocatalytic activity of TiO_2 nanotubes in this study was strongly influenced by irradiation time, which provides more photon energy to the photocatalytic materials. This study [40] shows that the duration of irradiation affects the percentage of degradation of methylene blue dye where the longer the irradiation time, the higher the rate of degradation. In our case, the rate of degradation efficiency has increased significantly in the first 20 minutes, and after 60 minutes the rate of degradation efficiency tends to be stable. This can be correlated with the fact that the longer irradiation time is applied, that is the UV light illumination on the resulted TiO_2 photocatalytic nanotubes, the more OH radicals are produced to get contact with methylene blue, and thus the greater the percentage of degradation efficiency can be obtained. Definitely, there is a saturation level for the OH radicals production during the UV light irradiation. The smaller bandgap energy of the TiO_2 nanotubes also contributes to the improved photocatalytic performance as in the case of post-hydrothermally treated samples at 150 °C as demonstrated in Fig. 12, *b*. Under this condition, an easier electron excitation from the valence band to the conduction band can facilitate the formation of more OH radicals for accelerated degradation of methylene blue.

It can be concluded that the synthesis of titanium dioxide nanotubes from a natural precursor, the mineral ilmenite, has been successfully carried out. In synthesizing titanium nanotubes through several stages, it has been successfully carried out, starting from the extraction of ilmenite through the hydrometallurgical process using the

sulfate pathway. Titanium oxosulphate is obtained, which will become the precursor for the following process. The second stage was also successfully carried out, namely the hydrolysis process, where titanium oxosulphate was given a heating treatment using water at 90 °C for 3 hours. Then the result will be obtained as a white precipitate in the form of TiO_2 particles. Scanning electron microscope (SEM) results show that the hydrolysis process results have successfully obtained TiO_2 nanoparticles (Fig. 1, *a*). The third stage was also successfully carried out, namely modifying the nanoparticles into TiO_2 nanotubes through a hydrothermal process at 150 °C for 24 hours. At this stage, the synthesis of TiO_2 nanotubes was successfully carried out from TiO_2 nanoparticles extracted from ilmenite, and this can be seen in Fig. 1, *b* with a nearly uniform tube morphology and TiO_2 nanotubes resulting from the hydrothermal process still have low crystallinity as shown from the XRD diffraction peaks that are still low (Fig. 7, *b*). The next step is carried out, namely the post-hydrothermal treatment stage, with the aim of increasing high crystallinity. In the fourth stage, it was also successfully carried out, namely increasing the crystallinity of TiO_2 nanotubes with several temperature variations from 80, 100, 120, and 150 °C. At this stage, it was successfully obtained that the increase in post-hydrothermal temperature to 150 °C succeeded in increasing the crystallinity significantly. The peak indicates this. The high XRD diffraction that can be seen in Fig. 7, *f* and post-hydrothermal treatment managed to maintain the integrity of the tube structure as shown from the morphology of TiO_2 nanotubes in Fig. 2, *d*. At this stage, the effect of increasing post-hydrothermal temperature resulted in a decrease in the bandgap energy of TiO_2 nanotubes up to 3.02 eV (Fig. 11, *e*) in contrast to the commercial precursor P25 Degussa TiO_2 nanotubes, which had bandgap energy above the bulk anatase TiO_2 of 3.20 eV. Photocatalytic tests carried out the results of the TiO_2 nanotubes produced in the last stage. At this final stage, a photocatalytic test was successfully carried out, which showed that the performance of TiO_2 nanotubes from ilmenite mineral precursors had the best degradation efficiency, as seen from the percentage of degradation efficiency in Fig. 12, *c*.

The limitations of this research are the low purity of TiO_2 nanoparticles extracted from ilmenite extraction. It is shown that TiO_2 nanoparticles still contain Fe impurities, the length of time for the hydrothermal process, and the absence of variations in NaOH concentration in the hydrothermal method. The drawback of this research is that there is no special treatment to purify TiO_2 nanoparticles extracted from ilmenite. This causes the percentage of titanium extraction to be still lower than 100 % so that in the process of synthesizing TiO_2 nanotubes, there are still Fe impurities. However, the successful synthesis of TiO_2 nanotubes with the mineral precursor ilmenite in this study can be used as a reference for further research with some improvements. In addition, this research can also provide knowledge that Indonesia has local natural resources of the mineral ilmenite, which contains titanium dioxide. Some improvements that can be used in further research are the use of adding iron powder (Fe) to control the formation of pure TiO_2 nanoparticles in the hydrolysis process of titanium oxosulphate ($TiOSO_4$) solution and being given special treatment before the hydrothermal method is carried out so that the hydrothermal process time can be reduced. The difficulty of reducing the hydrothermal processing time is because TiO_2 nanotube structures will not be formed when reducing the time. The process before the hydrothermal process must be carried out in this study. This is because it will save more energy. The post-hydrothermal method is the best method to increase the crystallinity of TiO_2 nanotubes, and ilmenite as a natural precursor to form TiO_2 nanotubes should be used in this study because its availability is still abundant.

7. Conclusions

1. In this research, TiO_2 nanotubes were sucessfully synthesized through wet-chemistry routes using ilmenite $FeTiO_3$ mineral. It was discovered that post-hydrothermal treatment at different temperatures of 80, 100, 120, and 150 °C facilitated the increase in the crystallite growth of the TiO_2 anatase phase from 19.19 to 25.76 nm while successfully maintaining the integrity of the hollow structure of the nanotubes. The increase in the temperature from 80 to 150 °C was also found to have decreased the bandgap energy values of the nanotubes from 3.33 to 3.02 eV. Moreover, the remaining sodium titanate phase, as well as the iron ion content in the nanotubes, also provides an advantage in reducing the bandgap energy of the TiO_2 phase.

2. The MB degradation test also showed that the synthesized nanotubes can provide good photocatalytic performance for the textile waste treatment with the best degradation efficiency of up to 97.11 % recorded with the nanotube sample post-hydrothermally treated at 150 °C.

Acknowledgments

The authors thank the Director of Research and Development and the Directorate of Research and Development, the University of Indonesia for funding this research through the International Indexed Publication Grant (PUTI Doctor) Year 2020 under contract number: BA-829/UN2. RST/PPM. 00.03.01/2020 as well as the Education Fund Management Institute (LPDP) of the Ministry of Foreign Affairs of the Republic of Indonesia for the fund provided through the Funding for Productive Innovative Research (RISPRO) Mandatory National Research Priority Theme (PRN) Part I with contract number: 83/ E1/PRN/2020. Our gratitude also goes to the reviewers for all the constructive feedback and comments.

References

1. Al-Mamun, M. R., Kader, S., Islam, M. S., Khan, M. Z. H. (2019). Photocatalytic activity improvement and application of UV-TiO_2 photocatalysis in textile wastewater treatment: A review. Journal of Environmental Chemical Engineering, 7 (5), 103248. doi: https://doi.org/10.1016/j.jece.2019.103248
2. Peralta-Zamora, P., Kunz, A., de Moraes, S. G., Pelegrini, R., de Campos Moleiro, P., Reyes, J., Duran, N. (1999). Degradation of reactive dyes I. A comparative study of ozonation, enzymatic and photochemical processes. Chemosphere, 38 (4), 835–852. doi: https://doi.org/10.1016/s0045-6535(98)00227-6

3. Gardiner, D. K., Borne, B. J. (1978). Textile Waste Waters: Treatment and Environmental Effects. Journal of the Society of Dyers and Colourists, 94 (8), 339–348. doi: https://doi.org/10.1111/j.1478-4408.1978.tb03420.x
4. Rafatullah, M., Sulaiman, O., Hashim, R., Ahmad, A. (2010). Adsorption of methylene blue on low-cost adsorbents: A review. Journal of Hazardous Materials, 177 (1-3), 70–80. doi: https://doi.org/10.1016/j.jhazmat.2009.12.047
5. Chen, D., Cheng, Y., Zhou, N., Chen, P., Wang, Y., Li, K. et. al. (2020). Photocatalytic degradation of organic pollutants using TiO_2-based photocatalysts: A review. Journal of Cleaner Production, 268, 121725. doi: https://doi.org/10.1016/j.jclepro.2020.121725
6. Humayun, M., Raziq, F., Khan, A., Luo, W. (2018). Modification strategies of TiO_2 for potential applications in photocatalysis: a critical review. Green Chemistry Letters and Reviews, 11 (2), 86–102. doi: https://doi.org/10.1080/17518253.2018.1440324
7. Nguyen, V. N., Nguyen, N. K. T., Nguyen, P. H. (2011). Hydrothermal synthesis of Fe-doped TiO_2 nanostructure photocatalyst. Advances in Natural Sciences: Nanoscience and Nanotechnology, 2 (3), 035014. doi: https://doi.org/10.1088/2043-6262/2/3/035014
8. Liu, N., Chen, X., Zhang, J., Schwank, J. W. (2014). A review on TiO_2-based nanotubes synthesized via hydrothermal method: Formation mechanism, structure modification, and photocatalytic applications. Catalysis Today, 225, 34–51. doi: https://doi.org/10.1016/j.cattod.2013.10.090
9. Vu, T. H. T., Au, H. T., Tran, L. T., Nguyen, T. M. T., Tran, T. T. T., Pham, M. T. et. al. (2014). Synthesis of titanium dioxide nanotubes via one-step dynamic hydrothermal process. Journal of Materials Science, 49 (16), 5617–5625. doi: https://doi.org/10.1007/s10853-014-8274-4
10. Kasuga, T., Hiramatsu, M., Hoson, A., Sekino, T., Niihara, K. (1999). Titania nanotubes prepared by chemical processing. Advanced Materials, 11 (15), 1307–1311. doi: https://doi.org/10.1002/(sici)1521-4095(199910)11:15<1307::aid-adma1307>3.0.co;2-h
11. Yuwono, A. H., Ferdiansyah, A., Sofyan, N., Kartini, I., Pujianto, T. H., Iskandar, F., Abdullah, M. (2011). TiO2 Nanotubes of Enhanced Nanocrystallinity and Well-Preserved Nanostructure by Pre-Annealing and Post-Hydrothermal Treatments. AIP Conference Proceedings. doi: https://doi.org/10.1063/1.3667246
12. Samal, S., Mohapatra, B. K., Mukherjee, P. S. (2010). The Effect of Heat Treatment on Titania Slag. Journal of Minerals and Materials Characterization and Engineering, 09 (09), 795–809. doi: https://doi.org/10.4236/jmmce.2010.99057
13. Subagja, R., Andriyah, L., Lalasari, L. H. (2013). Titanium Dissolution from Indonesian Ilmenite. International Journal of Basic & Applied Sciences IJBAS-IJENS, 13, 97–103. Available at: http://citeseerx.ist.psu.edu/viewdoc/download?doi=10.1.1.658.6995&rep=rep1&type=pdf
14. Mackey, T. S. (1994). Upgrading ilmenite into a high-grade synthetic rutile. JOM, 46 (4), 59–64. doi: https://doi.org/10.1007/bf03220676
15. Liang, B., Li, C., Zhang, C., Zhang, Y. (2005). Leaching kinetics of Panzhihua ilmenite in sulfuric acid. Hydrometallurgy, 76 (3-4), 173–179. doi: https://doi.org/10.1016/j.hydromet.2004.10.006
16. Ponaryadov, A. V., Kotova, O. B., Tihtih, M., Sun, S. (2020). Natural titanium dioxide nanotubes. Epitoanyag - Journal of Silicate Based and Composite Materials, 72 (5), 152–155. doi: https://doi.org/10.14382/epitoanyag-jsbcm.2020.25
17. Rohmawati, L., Istiqomah, Wulancahayani, E., Haefdea, A., Setyaningsih, W. (2020). Nanocrystaline Titanium Dioxide Nanotube (TDN) by Hydrothermal Method From Tulungagung Mineral Sand. Proceedings of the International Conference on Research and Academic Community Services (ICRACOS 2019). doi: https://doi.org/10.2991/icracos-19.2020.22
18. Ranjitha, A., Muthukumarasamy, N., Thambidurai, M., Velauthapillai, D., Agilan, S., Balasundaraprabhu, R. (2015). Effect of reaction time on the formation of TiO_2 nanotubes prepared by hydrothermal method. Optik, 126 (20), 2491–2494. doi: https://doi.org/10.1016/j.ijleo.2015.06.022
19. Camposeco, R., Castillo, S., Navarrete, J., Gomez, R. (2016). Synthesis, characterization and photocatalytic activity of TiO_2 nanostructures: Nanotubes, nanofibers, nanowires and nanoparticles. Catalysis Today, 266, 90–101. doi: https://doi.org/10.10160/j.cattod.2015.09.018
20. López Zavala, M. Á., Lozano Morales, S. A., Ávila-Santos, M. (2017). Synthesis of stable TiO_2 nanotubes: effect of hydrothermal treatment, acid washing and annealing temperature. Heliyon, 3 (11), e00456. doi: https://doi.org/10.1016/j.heliyon.2017.e00456
21. Zulfiqar, M., Omar, A. A., Chowdhury, S. (2016). Synthesis and characterization of single-layer TiO_2 nanotubes. Advanced Materials Research, 1133, 501–504. doi: https://doi.org/10.4028/www.scientific.net/amr.1133.501
22. Cullity, B. (1978). Elements of X-Ray Diffraction. Addison Wesley.
23. Tauc, J., Grigorovici, R., Vancu, A. (1966). Optical Properties and Electronic Structure of Amorphous Germanium. Physica Status Solidi (b), 15 (2), 627–637. doi: https://doi.org/10.1002/pssb.19660150224
24. Viet, P. V., Huy, T. H., You, S.-J., Hieu, L. V., Thi, C. M. (2018). Hydrothermal synthesis, characterization, and photocatalytic activity of silicon doped TiO_2 nanotubes. Superlattices and Microstructures, 123, 447–455. doi: https://doi.org/10.1016/j.spmi.2018.09.035
25. Kumar, K. V., Porkodi, K., Rocha, F. (2008). Langmuir–Hinshelwood kinetics – A theoretical study. Catalysis Communications, 9 (1), 82–84. doi: https://doi.org/10.1016/j.catcom.2007.05.019
26. Rezaee, M., Mousavi Khoie, S. M., Liu, K. H. (2011). The role of brookite in mechanical activation of anatase-to-rutile transformation of nanocrystalline TiO_2: An XRD and Raman spectroscopy investigation. CrystEngComm, 13 (16), 5055. doi: https://doi.org/10.1039/c1ce05185g
27. Yang, J., Jin, Z., Wang, X., Li, W., Zhang, J., Zhang, S. et. al. (2003). Study on composition, structure and formation process of nanotube $Na_2Ti_2O_4(OH)_2$. Dalton Transactions, 20, 3898. doi: https://doi.org/10.1039/b305585j

28. Yuwono, A. H., Sofyan, N., Kartini, I., Ferdiansyah, A., Pujianto, T. H. (2011). Nanocrystallinity enhancement of TiO_2 nanotubes by post-hydrothermal treatment. Advanced Materials Research, 277, 90–99. doi: https://doi.org/10.4028/www.scientific.net/amr.277.90
29. Djerdj, I., Tonejc, A. M. (2006). Structural investigations of nanocrystalline TiO_2 samples. Journal of Alloys and Compounds, 413 (1-2), 159–174. doi: https://doi.org/10.1016/j.jallcom.2005.02.105
30. Yuwono, A. H., Liu, B., Xue, J., Wang, J., Elim, H. I., Ji, W. et. al. (2004). Controlling the crystallinity and nonlinear optical properties of transparent TiO_2–PMMA nanohybrids. J. Mater. Chem., 14 (20), 2978–2987. doi: https://doi.org/10.1039/b403530e
31. An, Y., Li, Z., Xiang, H., Huang, Y., Shen, J. (2011). First-principle calculations for electronic structure and bonding properties in layered $Na_2Ti_3O_7$. Open Physics, 9 (6). doi: https://doi.org/10.2478/s11534-011-0072-x
32. Moradi, V., Jun, M. B. G., Blackburn, A., Herring, R. A. (2018). Significant improvement in visible light photocatalytic activity of Fe doped TiO_2 using an acid treatment process. Applied Surface Science, 427, 791–799. doi: https://doi.org/10.1016/j.apsusc.2017.09.017
33. Asiltürk, M., Sayılkan, F., Arpaç, E. (2009). Effect of Fe^{3+} ion doping to TiO_2 on the photocatalytic degradation of Malachite Green dye under UV and vis-irradiation. Journal of Photochemistry and Photobiology A: Chemistry, 203 (1), 64–71. doi: https://doi.org/10.1016/j.jphotochem.2008.12.021
34. Latifa, H., Yuwono, A. H., Firdiyono, F., Rochman, N. T., Harjanto, S., Suharno, B., (2013). Controlling the Nanostructural Characteristics of TiO_2 Nanoparticles Derived from Ilmenite Mineral of Bangka Island through Sulfuric Acid Route. Applied Mechanics and Materials, 391, 34–40. doi: https://doi.org/10.4028/www.scientific.net/amm.391.34
35. Chen, W., Guo, X., Zhang, S., Jin, Z. (2007). TEM study on the formation mechanism of sodium titanate nanotubes. Journal of Nanoparticle Research, 9 (6), 1173–1180. doi: https://doi.org/10.1007/s11051-006-9190-6
36. Morgan, D. L., Triani, G., Blackford, M. G., Raftery, N. A., Frost, R. L., Waclawik, E. R. (2011). Alkaline hydrothermal kinetics in titanate nanostructure formation. Journal of Materials Science, 46 (2), 548–557. doi: https://doi.org/10.1007/s10853-010-5016-0
37. Sreekantan, S., Wei, L. C. (2010). Study on the formation and photocatalytic activity of titanate nanotubes synthesized via hydrothermal method. Journal of Alloys and Compounds, 490 (1-2), 436–442. doi: https://doi.org/10.1016/j.jallcom.2009.10.030
38. Kotani, Y., Matsuda, A., Kogure, T., Tatsumisago, M., Minami, T. (2001). Effects of Addition of Poly(ethylene glycol) on the Formation of Anatase Nanocrystals in SiO_2–TiO_2 Gel Films with Hot Water Treatment. Chemistry of Materials, 13 (6), 2144–2149. doi: https://doi.org/10.1021/cm001419r
39. Wang, L.-Q., Baer, D. R., Engelhard, M. H., Shultz, A. N. (1995). The adsorption of liquid and vapor water on TiO_2(110) surfaces: the role of defects. Surface Science, 344 (3), 237–250. doi: https://doi.org/10.1016/0039-6028(95)00859-4
40. Reza, K. M., Kurny, A., Gulshan, F. (2015). Parameters affecting the photocatalytic degradation of dyes using TiO_2: a review. Applied Water Science, 7 (4), 1569–1578. doi: https://doi.org/10.1007/s13201-015-0367-y